ORIGINAL RESEARCH ARTICLE

Investigation of Microstructural and Electrochemical Behavior of Chromized-Doped Layers with Variant Magnesium Concentrations

SARRA DJEMMAH[1,2*], MICHEL VOUÉ[2], YOUCEF MADI[1], DJILALI ALLOU[3], AHMED HADDAD[3], and HAMIDA BOUCHAFAA[4]

[1]University of Science and Technology Houari Boumediene, Laboratory of Technology of Materials (LTM), Algier 1 6111, Algeria.
[2] University of Mons, Physics of Materials and Optics Unit (LPMO), Research Institute for Materials Science and Engineering, Mons7000,Belgium.
[3]Research Center in Industrial Technologies (CRTI), Algiers16014,Algeria.
[4]University of Science and Technology Houari Boumediene, Laboratory of Material Science and Engineering (LSGM), Algiers16111, Algeria.
E-mail: sdjemmah@usthb.dz

Abstract. This study provides an innovative approach about chromized-doped layers by discovering the optimal proportion of Mg (namely, 1wt%, 2wt%, and 3wt%) to use as doping elements in order to enhance diffusion and stabilize the formed chromium oxide during the diffusion process. Our main objective is to evaluate the effect of Mg doping on the microstructural, the electrochemical behavior of the doped layer, systematically evaluating the impact of simultaneous variation of NH_4Cl activator. The chromized-doped layers were analyzed by X-ray diffraction (XRD) and a scanning electron microscopy (SEM) equipped with EDX analysis. The doped layers were tested in 3.5 % NaCl solution, and then were characterized by electron probe micro-analyzer (EPMA). The results revealed that doping contributed to the improvement of chromium diffusion for all the layers (≥ 96 % Cr), stabilizing chromium oxide by forming a more stable oxide ($MgCr_2O_4$). However, Cr-Mg/1wt.% showed the most homogenous crystalline structure and topography compared to the other layers, with the most insignificant defects. The Cr-Mg/1 wt.% presented an excellent corrosion resistance in the 3.5 %NaCl solution, where its surface did not suffer of any type of corrosion or damages. In addition, the balanced value of the activator (NH_4Cl) relative to the other doped layers may play a role. As a result, the Cr-Mg doped with 1 wt.% (with 4 wt.% NH_4Cl) could be a robust and innovative surface, paving the way for new possibilities in the field of chromizing coatings.

Keywords. chromized-doped; Mg; Doping; Chromizing; Microstructural; Electrochemical behavior.

1. Introduction

One promising approach for mitigating corrosion, wear, and damage on surfaces involves the application of chromium coatings through a high-temperature diffusion technique known as the chromizing process [1]. Chromizing process, characterized by the diffusion of chromium into the steel matrix at specific temperatures determined by phase equilibrium diagrams (binary and ternary) and carbon content [2], which it results in the formation of a chromium-rich surface layer. This layer acts as a crucial reservoir, reinforcing resistance and preserving the underlying steel's integrity. In the face of corrosion, oxygen exposure, or damage, the diffused chromium reacts by creating a protective barrier of chromium oxide (Cr_2O_3), without depleting the chromium in the base steel. It may occur at different temperatures and with the exposure to aggressive chemicals agents in the manufacture of chemical processing equipment or components used in petrochemical refineries, nuclear central for example [3]. An unstable Cr_2O_3 formed layer in such conditions might lead to rapid degradation result in the formation of microstructural defects, pores, and cracks, compromising the protective barrier [4]. This would leave the underlying material susceptible to rapid aggressive corrosive attack, potentially leading to premature failure of the equipment or components.

Challenges encountered in the chromizing process include impurities, pores, cracks, particles on the surface, and the formation of chromium carbides such as $Cr_{23}C_6$, Cr_7C_3, and Cr_3C_2 [5, 6]. While selecting low-carbon steel reduces the probability of chromium carbide formation, it remains a challenge due to the carbon affinity for chromium element. The high reactivity of chromium at elevated temperatures during the diffusion process accelerates the formation of chromium carbides [7, 8], enhancing wear, hardness, and corrosion resistance but compromising surface flexibility and make it brittle, weak, prone to cracking and peeling [9]. However, minority phase of chromium oxide may be attainable during the chromizing treatment, but potentially exhibiting nonhomogeneous and instability microstructure [10]. As the non-stable chromium oxide that could be formed in the several environmental conditions, which it develops in a fragile and unproductive way. In spite of this, it could prevent and decrease the formation of chromium carbides and impurities during the process.

In this context, doping the chromized-layer with a stable thermodynamically elements is one of the promote solution to stabilize the minority chromium oxide that could be formed and enhance the α-iron phase at high temperatures during the diffusion process [11, 12]. For instance, it was found that adding magnesium as doping element offers the possibility of stabilizing chromium oxide [13], which could also accelerate

surface chromium diffusion and inhibit chromium carbide formation [14]. Magnesium doping can improve deformation resistance, increase hardness, roughness through grain refinement, and play a crucial role in enhancing corrosion resistance [12]. There are, however, issues that should to be resolved, and that is the concentration of magnesium in the pack mixture. This necessity arises from the observed phenomenon where, at oxygen pressures proximal to atmospheric conditions, dissolved Mg in temperature range between 400 °C and 1200 °C induces the creation of electron holes to offset its presence. Conversely, under significantly reduced oxygen activities, the compensatory mechanisms involve the formation of oxygen vacancies or possibly interstitial chromium ions [15]. Varying proportions of Mg may exert influence on these compensatory processes, underscoring the critical importance of Magnesium quantity control for ensuring consistency in results within the high-temperature chromium coating. Additionally, Acra et al [16], they found that it is possible to achieve improvement in properties by utilizing a lower content of magnesium. On the other hand, it is known that the chromizing process is sensitive; altering an element in the powder mixture can yield significantly different result. Studies performed by Chen et al [17], have highlighted the importance of balanced amounts of the ammonium chloride activator (NH_4Cl) in modulating the growth rate and diffusion of chromized layers. Furthermore, it implies that the surface diffusion rate can be slowed at a reduced concentration of the used activator, allowing adjacent grains to coalesce and larger grain structures to develop in the chromized layer. In addition, in studies conducted by Park et al. [18], they found that low concentration of the activator NH_4Cl, could affect the thickness and interdiffusion zone.

Based on our investigations, previous research has not yet addressed the influence of varying doping magnesium content on the chromizing by cementation pack process, in order to optimize the parameters required for a stable chromium layer with low formation of defects and carbides. However, the novelty in our work lies in the precise control and systematic variation of magnesium content within the chromizing powder mixture exploring its impact on the quality of the produced layer. Moreover, it delves into the nuanced role of magnesium content in stabilizing the formed chromium oxide (Cr_2O_3), which could enhance chromium diffusion. Nevertheless, variation in magnesium concentration will systematically cause a variation in the activator (ammonium chloride; NH_4Cl) values that have been used in the powder mixture, enabling us to examine its impact on the microstructural and electrochemical behavior when it is employed with Magnesium.

2. Experimental Section

2.1. Chromizing-Doping Process

In this experiment, the substrate of choice is AISI 430 ferritic stainless steel, characterized by its composition of 16% Cr (chromium) and its low carbon content of about 0.06 %C. Before preceding the chromizing treatment, the surface of the AISI 430 stainless steel substrate was carefully polished to an almost smooth finish using an abrasive paper (#1200). To ensure the removal of any contaminants and impurities, the polished substrate underwent a thorough cleaning process. This cleaning procedure involved immersing the substrate in an ultrasonic bath filled with an ethanol solution for duration of 5 minutes. For doping the substrate with magnesium (Mg), the chromizing process in pack cementation was used. However, each specimen (substrate of 430 SS) was carefully placed within an alumina crucible containing a specific pack mixture and a lid. The alumina crucibles were chosen for their resistance to high temperatures (up to1800°C). The doping with chromizing process entailed immersion of the specimens in a pack mixture comprising chromium (Cr), ammonium chloride (NH_4Cl), Alumina (Al_2O_3) and magnesium (Mg). The weight ratio of these components and the chromizing conditions for doping the substrate are regrouped in Table 1. It can be seen from the Table 1, that the magnesium value increased by 1 wt.%, 2 wt.% and 3 wt.%, while the value of the activator (NH_4Cl) decreased to 2 wt.%.

The production of chromized-doped layers was carried out at a temperature of 1050°C, using a ramp rate of 6°C/min, in a horizontal Carbolite GHC tube furnace (Carbolite TZF 12/100/-900, Hope Valley, UK). The tubular furnace is composed of several key elements, allowing precise control of the temperature used inside the inner pipe, where the systems (crucible + specimen + pack mixture) were placed. On the other hand, the thermal cycle used consisted of several distinct stages. Firstly, an injection of approximately 2 bar of argon (Ar) was introduced into the inner pipe to prevent any undesirable reactions that may occur during the chromizing doping process. A flow rate of approximately 2 L/min was maintained to evacuate the entire total volume (of about 1800 cm^3). At this stage, the system is maintained at an ambient temperature, implying that no external heating is required. Furthermore, both ends of the inner tube remain open to allow oxygen and non-protective gases to escape from within the furnace. Then, the inner tube inlets were sealed to initiate the preheating of the system. The temperature was initially set at 50°C and maintained at this level for duration of one hour. This step serves the purpose of preheating the alumina crucible and the systems (pack mixture + specimen) before reaching the treatment temperature. Finally, the temperature was gradually increased to 1050°C (ramp rate of 6°C/min), and then maintained at this temperature for 8h (Table 1). In this phase, the system remained closed and under control (presence of argon). In addition, cooling must also take place in a closed controlled environment, under injection of argon (Ar) to maintain inert conditions and avoid any possible contamination during the cooling process.

Table 1

Component weight ratio (wt. %) for the chromizing-doping process at 1050°C using cementation pack.

	Component (wt.%)				Working conditions
	Cr	**NH_4Cl**	**Al_2O_3**	**Mg**	
Cr-Mg/1 wt.%	20	4	70	**1**	T = 1050 °C
Cr-Mg/2 wt.%	20	3	70	**2**	
Cr-Mg/3 wt.%	20	2	70	**3**	t = 8 h

2.2. Microstructural Characterization

To identify the phase composition and the crystalline structure formed after doping the substrates, an XRD analysis was conducted using a Siemens diffractometer (Siemens D500 diffractometer, Munich, Germany) with Cu-Kα radiation (λ= 1.5406 Å), in the 2θ range from 30° to 110°. On the other hand, the topography of doped surfaces was analyzed by scanning electron microscope (SEM) type Zeiss LEO 1455VP(Oxford instr-ument and INCA software, London, UK), under an acceleration voltage of approximately 20kV.Furthermore, an energy dispersive X-ray spectrometer (EDX), Inca X by Oxford instruments is coupled with the SEM analyzer. The investigation focuses on tracking the diffusion of chromium (Cr), the incorporation of oxygen, and the interdiffusion of iron (Fe) and carbon (C) within the matrix through internal and/or external diffusion phenomena. In addition, SEM and EDX analysis could offer higher resolution in larger scales to evaluate the crystal structure and irregularities on the doped-coated surfaces.

2.3. Electrochemical Testing

The experimental part of the study involves electrochemical corrosion testing using a 3.5% sodium chloride (NaCl) solution to assess corrosion resistance and electrochemical behavior under conditions simulating saline environments where the layer could be exposed. However, a 3.5% NaCl electrolyte solution was prepared by dissolving sodium chloride in distilled water at room temperature (± 25 °C) with agitation (for 24h).Sodium chloride is commonly used to simulate corrosive environments due to the aggressive chloride ions (Cl^-) it replicates and the presence of sodium ions (Na^+). Chloride ions (Cl^-) can cause localized corrosion, in particular aggressive corrosion in the form of deep pitting.

Chromized-doped surfaces were immersed in the 3.5% NaCl solution, where they were scanned over a potential range of about -1000 mV to 1000 mV using scan rate of 1 mV/s, by a Metrohm autolab (Potensiostat Parstat 3000A-DX, DX, Princeton Applied Research, USA) connected to an electrochemical cell. As part of this test, three electrodes were immersed in 3.5% NaCl solution: a working electrode as coating's surface, an Ag/AgCl as a reference electrode, and a Pt foil counter electrode. A potential difference was established between these electrodes, creating an electrical circuit, where the electrochemical reactions occur at the electrode-solution interface, generating measurable electric currents after closing the circuit. These reactions are essential for understanding and studying corrosion, electrochemical reaction kinetics, and determining the energy storage capacity of coated surfaces. After polarization the immerged Surfaces in 3.5 % NaCl were characterized by an electron probe microanalysis (EMPA, JEOL, JXA-8230,Tokyo, Japan) under an electronic analysis energy of 10 keV. Thus, morphology and elemental analysis of corrosion products formed on the tested surfaces in a 3.5 % solution were deduced and investigated. The formed products were studied using different excitation potentials (Kα1 transitions of Cr, O, Cl, Na, C, N, and Fe).

3. Results and Discussion

3.1. Microstructural Investigations

The thickness of the doped coatings was evaluated to derive a quantitative relationship between the developed thicknesses (µm), Mg content (wt.%) , growth rate ($nm.min^{-1}$); hence the results are represented in the Table 2.

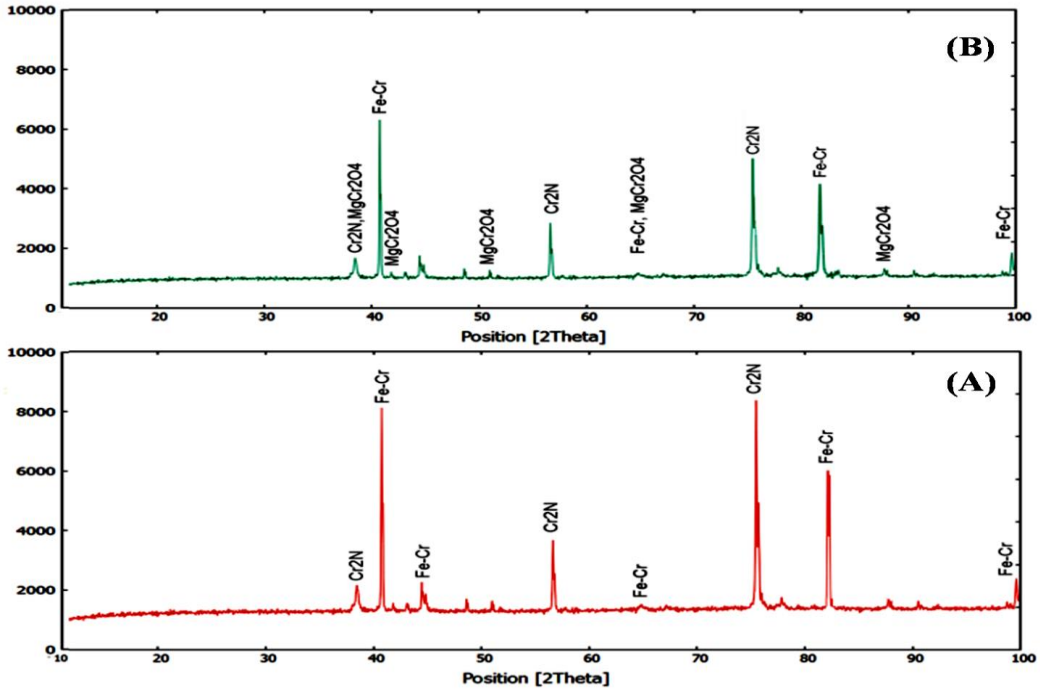

Fig.1. X-ray diffraction (XRD) spectra of Mg-doped coatings: (1) doped with 1 wt.% Mg-doped; (2) doped with 2wt.% and 3 wt.% Mg.

The growth rate, typically measured in nm/min, can be calculated and estimated using the following equation:

$$GR=d/t$$

Where (d) is the thickness of the layer, and (t) is the processing time.

The results show that the variation in thickness of the doped layers as a function of Mg content in the pack mixture is related to the growth rate. Nevertheless, it should be noted that the thickness values ranged from 24 µm to 26 µm, where the coating doped with 2 wt.% Mg exhibited a highest value for both thickness (26.16 µm) and growth rate (54.25nm/min).An average difference of 2 $nm.min^{-1}$ in growth rate for the Cr-Mg layer doped with 3 wt.%, suggests that variation in Mg content could influence on both growth rate and thickness. Whereas, Wen et al [19], in their work, they found that insufficient activator addition can result in unsatisfactory thickness of the coated layer. This could justify the lowest growth rate value of the Cr-Mg/ 3 wt.%, considering that the powder mixture used for this layer contained the lowest activator concentration (NH_4Cl, 2 wt.%) compared to the other employed powder mixtures. In the studies conducted by Park et al. [18], concerning the impact of varying the NH_4Cl activator agent, where their findings indicate that a low concentration of NH_4Cl activator could lead to the formation of precipitates within the inter-diffusion zone. A layer with increased thickness irregularities and non-uniform distribution may result from this doping process.

X-ray diffraction analyses were conducted to identify the resulting phases after Mg doping process. All the three chromized-doped coatings exhibited significant results concerning the solid solution of iron-chromium (Fe- Cr) phase, which intense peaks can be observed in X-ray diffraction patterns (Fig. 1), indicating the diffusion of chromium into the coated surface matrix at the depth. Previous research has already established that the ferritic phase (α) remains stable at the temperature of 1050 °C in the ferritic stainless steel.

Table 2

Variations in thickness and growth rate of Cr-doped layer as function of Mg concentration (wt.%).

Coating	Thickness (µm)	Growth rate ($nm.min^{-1}$)
Cr -Mg/ 1 wt.%	25.42 ± 1	53.70
Cr -Mg/ 2 wt.%	26.16 ± 1	54.25
Cr -Mg/ 3 wt.%	24.75 ± 1	51.56

Additionally, the presence of chromium nitride (Cr_2N) in the doped coatings can be noticed, suggesting that doping did not adverse significant impact on the formation of the nitrides chromium phase. Moreover, the Cr-Mg/ 1 wt.% doped coating showed prominent Fe-Cr peaks , as in Fig. 1-A. However, in the doped coating Cr-Mg/ 2 wt.% and Cr-Mg/ 3 wt.% distinct observations were noted, where both coatings exhibited similar X-ray diffraction results, as illustrated in Fig. 1-B. The formation of $MgCr_2O_4$ oxide is evident from the detected low-intensity peaks (minority phase formation), while those peaks corresponding to $MgCr_2O_4$ phase were not detected in the analysis of the doped Cr-Mg/1 wt.%. One possible explanation for this observation is that the reduced presence of ammonium chloride (NH_4Cl) has a noticeable effect on the diffusion reaction during diffusion process. This reduction slows down the reaction, allowing the formation of chromium oxide (Cr_2O_3) in minority phase, which it is justified by the limited presence of of oxygen in the powder mixture. Then, the formed magnesium oxide (MgO) during the diffusion process and the

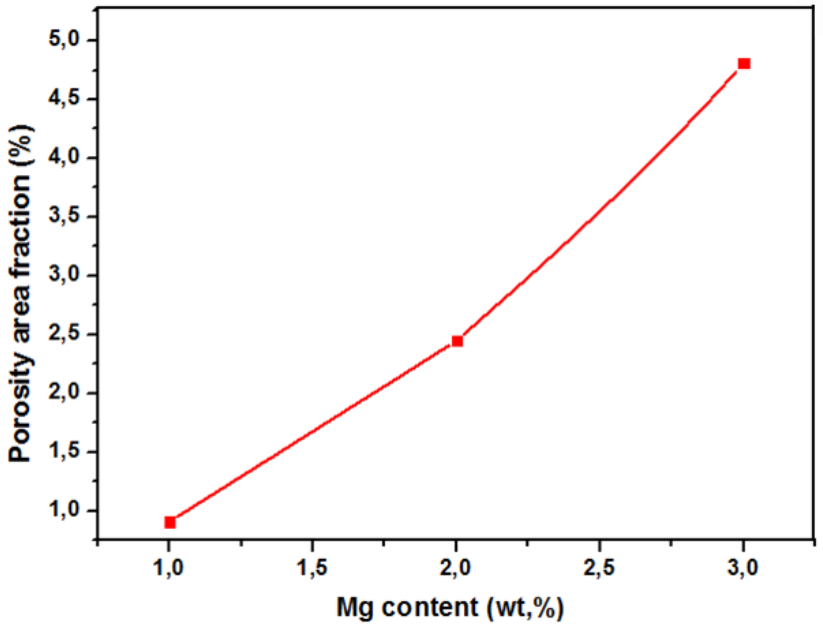

Fig. 2. SEM Micrograph and EDX analysis of the chromized-doped surface with 1 wt.% of Mg.

Nitrogen (N) decomposed formed chromium oxide (Cr_2O_3), allowing the formation of $MgCr_2O_4$ oxide in very minority phase, which it is considered as a more stable phase ($MgCr_2O_4$) than the Cr_2O_3 phase. Therefore, it could enhance hardness and corrosion resistance [20]. Further, the formation of $MgCr_2O_4$ oxide could serve as a barrier against the rapid development of chromium oxide during high temperature diffusion, since Cr_2O_3 oxide can rapidly consume chromium and disrupt chromium diffusion. Due to this, the chromium content of the mixte chromized layer; containing a minority phase of Cr_2O_3 is below 75 % in the previous study [11]. Studies by Wang and Liu et. Al. [20], have shown that $MgCr_2O_4$ formed oxide is primarily composed of magnesium oxide (MgO) and chromium oxide (Cr_2O_3). In research conducted by Fedorchenko et al. [21], magnesium was found to be an active agent in the reaction, absorbing nitrogen to form a stable oxide of $MgCr_2O_4$with chromium oxide (Cr_2O_3). No chromium carbides were detected in X-ray analysis, confirming the success of the chromium diffusion, the elimination of impurities and the reduction of oxygen during the process.

Topography and elemental analysis were conducted on all the chromized-doped surfaces using a scanning electron microscope (SEM) coupled with an energy dispersive X-ray (EDX). Additionally, the variation of surface porosity level as a function of Mg content was also quantified from the taken SEM images (high resolution). The results are presented in Fig. 2, 3, 4 and 5. Microscopic analysis of the chromized-doped surfaces revealed a denser crystalline morphology, where structure's grain size widened with increasing of Magnesium content. Overall, pores were observed within all the doped- layers, where the Cr-Mg/1 wt.% layer showed a small and narrow pore, which could be insignificant in the layer (Fig.3).The formation of pores could be attributed to inter-diffusion phenomena ; leading to the kirkendall effect, confirming that the inter-diffusion of chromium was not limited [17]. Based on the results displayed in Fig.2, the surface of the doped 1 wt.% Mg often has a low porosity level (< 1.0%), while increasing the Mg content in the powder mixture lead to the increase in the level of the surface porosity. To further analyze these coatings, linear EDX analysis was conducted using chromium K-line, iron K-line and oxygen K-line. The results revealed a prominent chromium (Cr) peak in all the doped coatings, confirming the deposition of chromium (Cr) on the surface through the chromizing process, which it results in high chromium rich regions. We observed a predominant chromium concentration of 98.15% in the EDX analysis of the Cr-Mg/1 wt.% doped coating (Fig. 3), which represents a significant result compared to previous studies. Simultaneously, minor peaks of oxygen (0.08%) were detected. Surface chromium concentrations for the chromizing layer produced by pack cementation typically range between 50% and 60%, rarely reaching 70%. When measuring the average chromium concentration across the coating thickness, this concentration is actually much lower when using NH_4Cl as an activator of the diffusion reactions [2]. As the Mg content increase, an appearance of non-crystalline structure zones containing a porosity network can be observed. These non crystalline areas were analyzed to better understand the nature of the resulted elements after chromizing process, performing linear

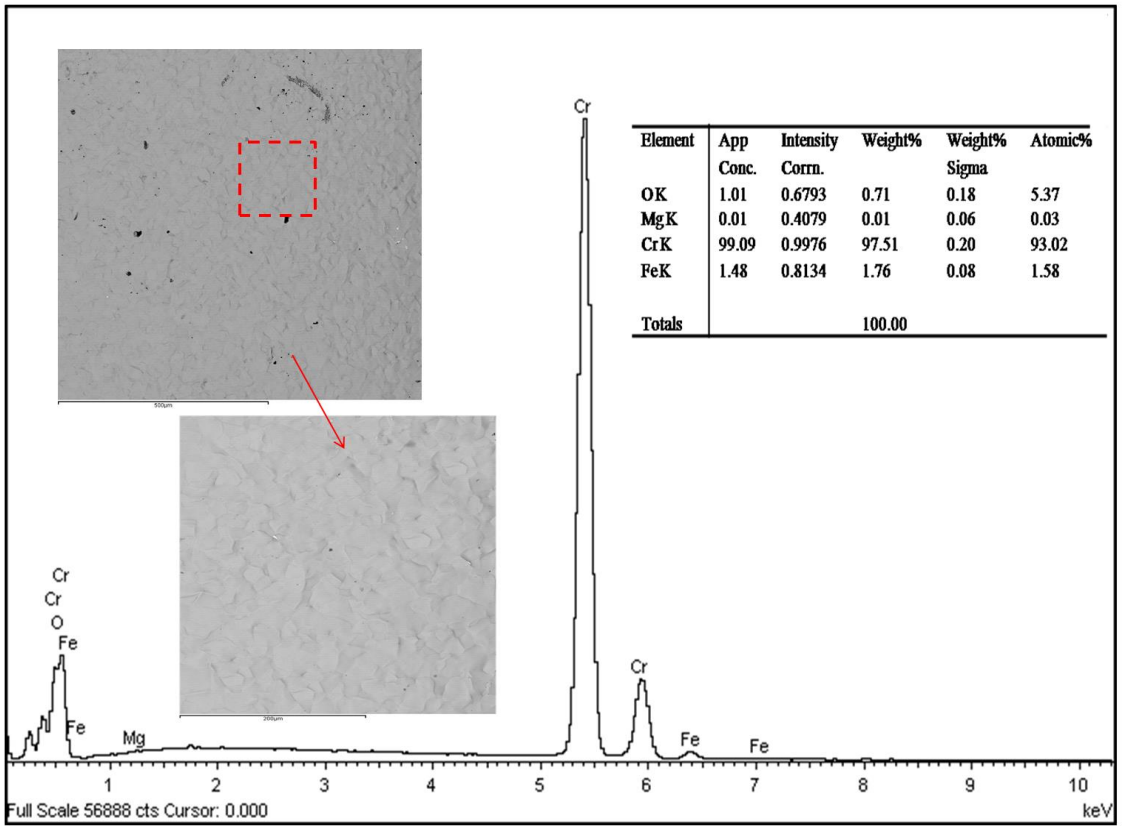

Element	App Conc.	Intensity Corrn.	Weight%	Weight% Sigma	Atomic%
OK	1.01	0.6793	0.71	0.18	5.37
MgK	0.01	0.4079	0.01	0.06	0.03
CrK	99.09	0.9976	97.51	0.20	93.02
FeK	1.48	0.8134	1.76	0.08	1.58
Totals			100.00		

Fig. 3. SEM Micrograph and EDX analysis of the chromized-doped surface with 1 wt.% of Mg.

EDX analysis in two different spots, namely spot (1) and spot (2), as illustrated in Fig. 4-A, B and Fig. 5-A, B. A high diffusion of chromium was confirmed for the doped coatings Cr Mg/2 wt.% and Cr-Mg/3 wt.% (intense peaks), where their surface were reached 96 and 95, respectively. However, this result was detected in the crystalline area, in spot (1) (Fig. 4-A and Fig. 5-A). On the other hand, the region with non-crystalline structure (spot 2) as illustrated in the Fig. 4-B and Fig. 5-B, could represent the formation of $MgCr_2O_4$ oxide, which it is supported by the reduction in chromium content from the EDX analysis compared to the crystalline region yielding a low values of about 85.15% and 55.36 % for coatings doped with 2 wt.% Mg and 3 wt.% Mg, respectively Consequently, the increase in magnesium content to 3 wt.%, in the used powder mixture could lead to a slower interdiffusion reactions due to the decreased of the ammonium chloride (NH_4Cl) content (2 wt.%). This result was not observed in the EDX analysis of the Cr- Mg/1 wt.% chromized-doped coating (Fig.3), which may be attributed to the balanced mass system between magnesium and ammonium chloride in the powder mixture. In addition, the formation of chromium oxide was not observed on the surface of this coating, where it revealed high surface chromium concentration and an improved diffusion. For further information, an in-depth analysis was conducted by performing concentration profiles of elements – iron (FeK), chrome (CrK), Nitrogen (NK) and oxygen (OK) – in order to follow the evolution of these elements through the chromized-doped surfaces and to assess the chromium concentration in the matrix. Thus relate it to the X-ray diffraction results illustrated in Fig.1. The Fig. 6 illustrates concentration profiles and topography of the interfaces of the different doped coatings. The results reveal that all the interfaces consist of two layers: an upper (outer layer) and a lower (inner layer), each with distinct characteristics. However, we can notice the formation of porosities network at the interface of the coating doped with Cr-Mg/2 wt.% doped-chromized , where they developed in the interface of the Cr-Mg/3 wt.% doped-chromized (Fig. 6-C), a phenomenon that was not observed in the coating doped with 1 wt.% Mg (Fig. 6-A). Additionally, Cr-Mg/1 wt.% exhibits the most favorable chromium diffusion properties into the substrate matrix. As we delve into the matrix, a chromium concentration of 32.46 % was identified into the matrix where no trace of oxygen (O) was detected. In contrast, the Cr- Mg/2 wt.% and Cr-Mg/3 wt.% show a chromium concentration about 30.85% and 29.46%, respectively. An increase in oxygen (O) concentration as the doping element's content increases was also observed in the profiles analysis. Furthermore, a low trace of nitrogen (N) (low concentration) was detected for all the coatings, confirming the presence of chromium nitrides (Cr_2N) as it was identified previously by the X-ray analysis (showed in Fig. 1). The chromium nitride (Cr_2N) is found to slightly decrease with the increase of the Mg content in the powder mixture (decreased activator content). Nevertheless, Mg doping element may enhance chromium diffusion through this chromizing process and demonstrates higher and significant matrix concentrations compared to the chromium coating non doped produced by the

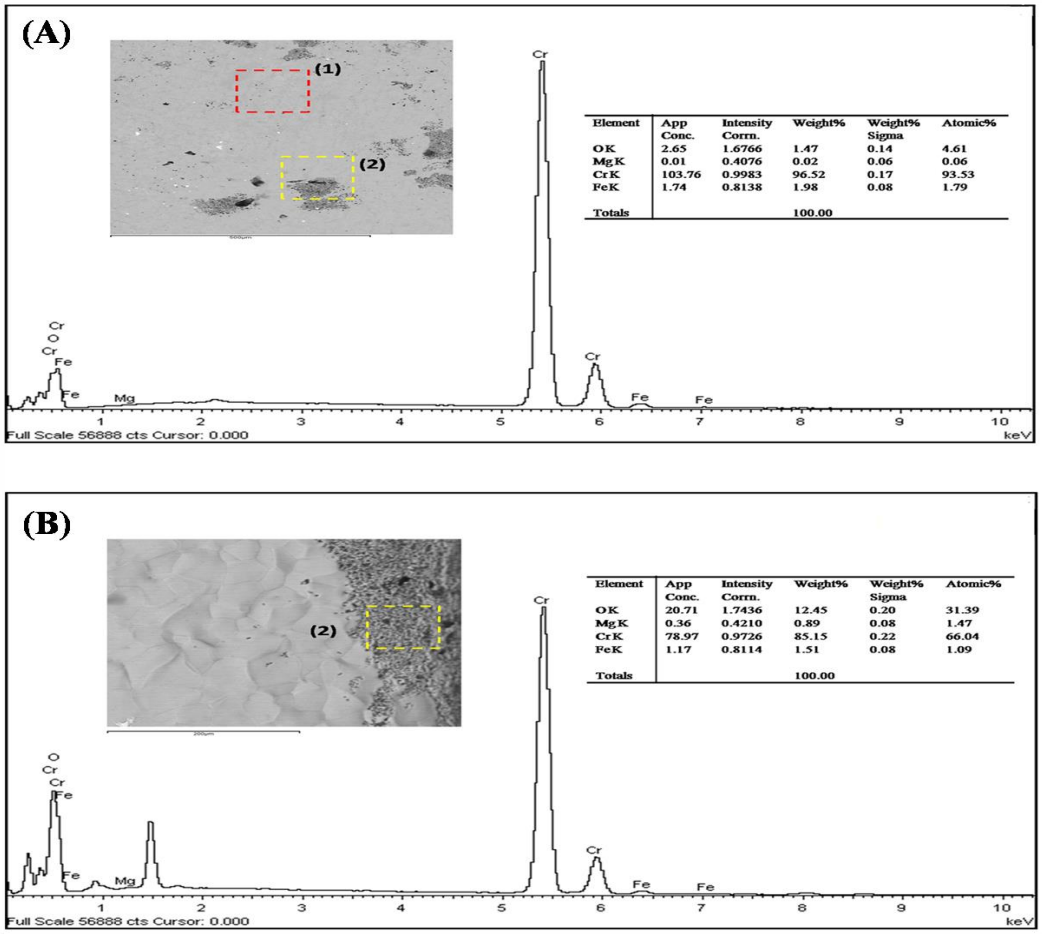

Fig. 4. SEM Micrograph and EDX analysis of the coated surface doped with 2 wt.% Mg: (A) Analysis in spot 1; (B) Analysis in spot 2.

same process, where this layer usually presented a diffused chromium content less than 20 % in the matrix [2, 11]. This could be justified by the ferritic structure of employed AISI 430 steel, which remains stable during the elevated temperature treatment and exhibits enhanced chromium atom mobility, within its structure.

3. 2. Electrochemical Behavior

Fig. 7 shows the potentiodynamic polarization curves for the surfaces of the chromized-doped coatings subjected to electrochemical tests in a 3.5% NaCl solution. We can notice a significant improvement in the corrosion resistance of the surfaces after doping the chromized layer (Fig. 7-Curve 2). Generally, a higher corrosion potential (E_{corr}) and a lower corrosion current (I_{corr}) values result in enhanced corrosion protection performance [22]. Analyzing the polarization curves plotted in Fig. 7 and the electrochemical data summarized in Table 3, it becomes apparent that corrosion potential (E_{corr}) of the doped Cr-Mg coatings tends to have fewer negative values, leading to smaller corrosion current values (I_{corr}). However, the surface of Cr-Mg/ 1 wt.% exhibits less negative corrosion potential (E_{corr}) values about of -52.16 mV compared to the other chromized-doped coatings (even to the chromized surface without Mg doping, illustrated in Fig. 7-curve 2), accompanied by a nominal corrosion current density (Icorr) of 0.03 µA/cm².

In contrast, increasing the Mg content to 2 wt.% and 3 wt.% results in more negative corrosion potential values (reaching -157.29 mV and -178.18 mV, respectively) with a concurrent increase in the corrosion current density (0.08 µA/cm² and 0.219 µA/cm², respectively). In line with the DoE experimental design methodology [23], achieving improved corrosion resistance in a specific environment could be ensured by targeting corrosion current density coefficient (I_{corr}) below 1 µA/cm². In addition, these results indicate that the coating Cr-Mg/ 1 wt.% exhibits significantly higher resistance than the other doped coatings in terms of the parameters of E_{corr}, I_{corr}, and the constant βa (241.51 mV/dec), which could be attributed to the high chromium content on the surface and in the matrix, also, to the absence of significant defects (porosity and voids), as has already been noted for the other chromized-doped illustrated in the Fig.4 and Fig.5. Electrochemical impedance spectroscopy (EIS) measurements were also conducted to assess the impact of doping on the corrosion rate of the doped-chromized layers. Fig.8 presents Nyquist plot representations of impedance diagrams and the electrochemical circuit. Upon the incorporation of Mg, an observed expansion of the capacitive semicircles was noted. As a result, the capacitive arcs become larger. This suggests a likely slowdown in the corrosion rate and the resistance behavior. Therefore, this alteration may result from a spontaneous passivation phenomenon, where a protective layer forms, acting as a barrier that prevents aggressive chloride ions (Cl^-) from penetrating and initiating the propagation of corrosion. On the other hand, the protective doped layer in this

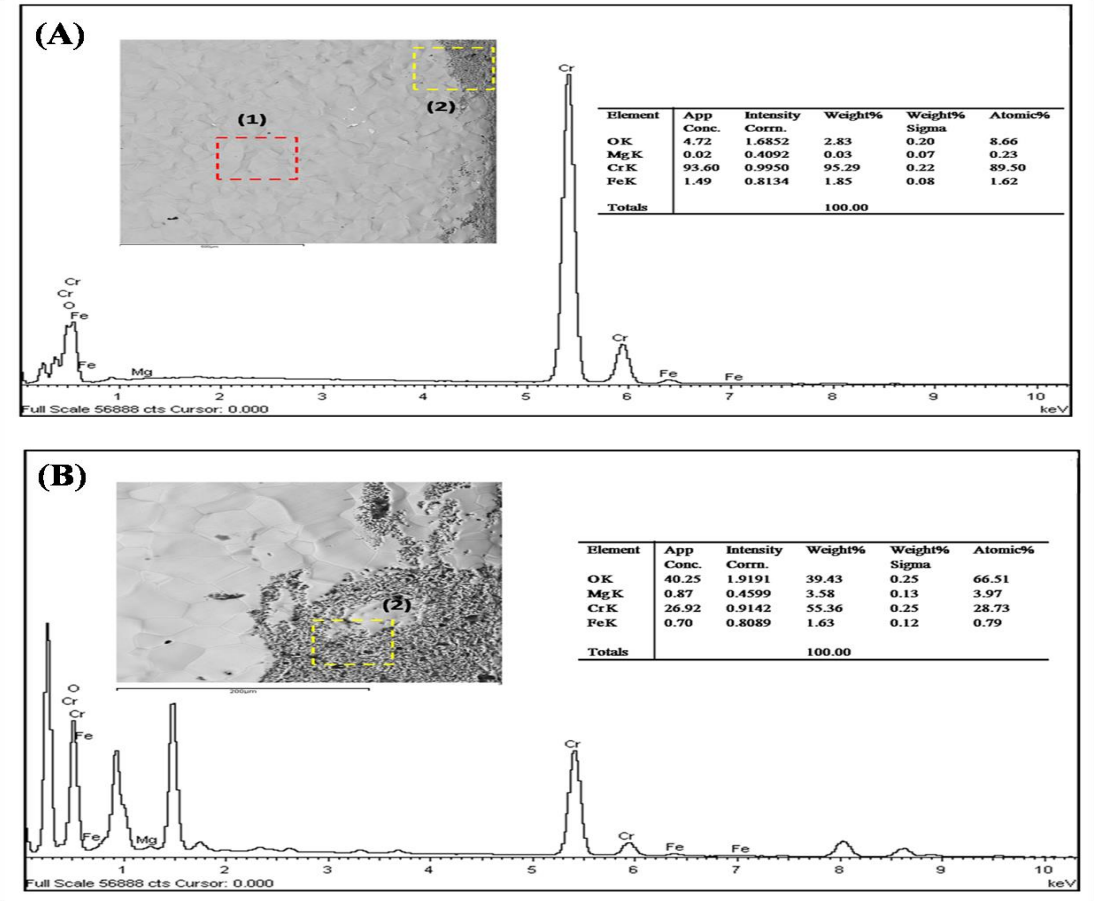

Fig. 5. SEM Micrograph and EDX analysis of the coated surface doped with 3wt.% Mg: (A) Analysis in spot 1; (B) Analysis in spot 2.

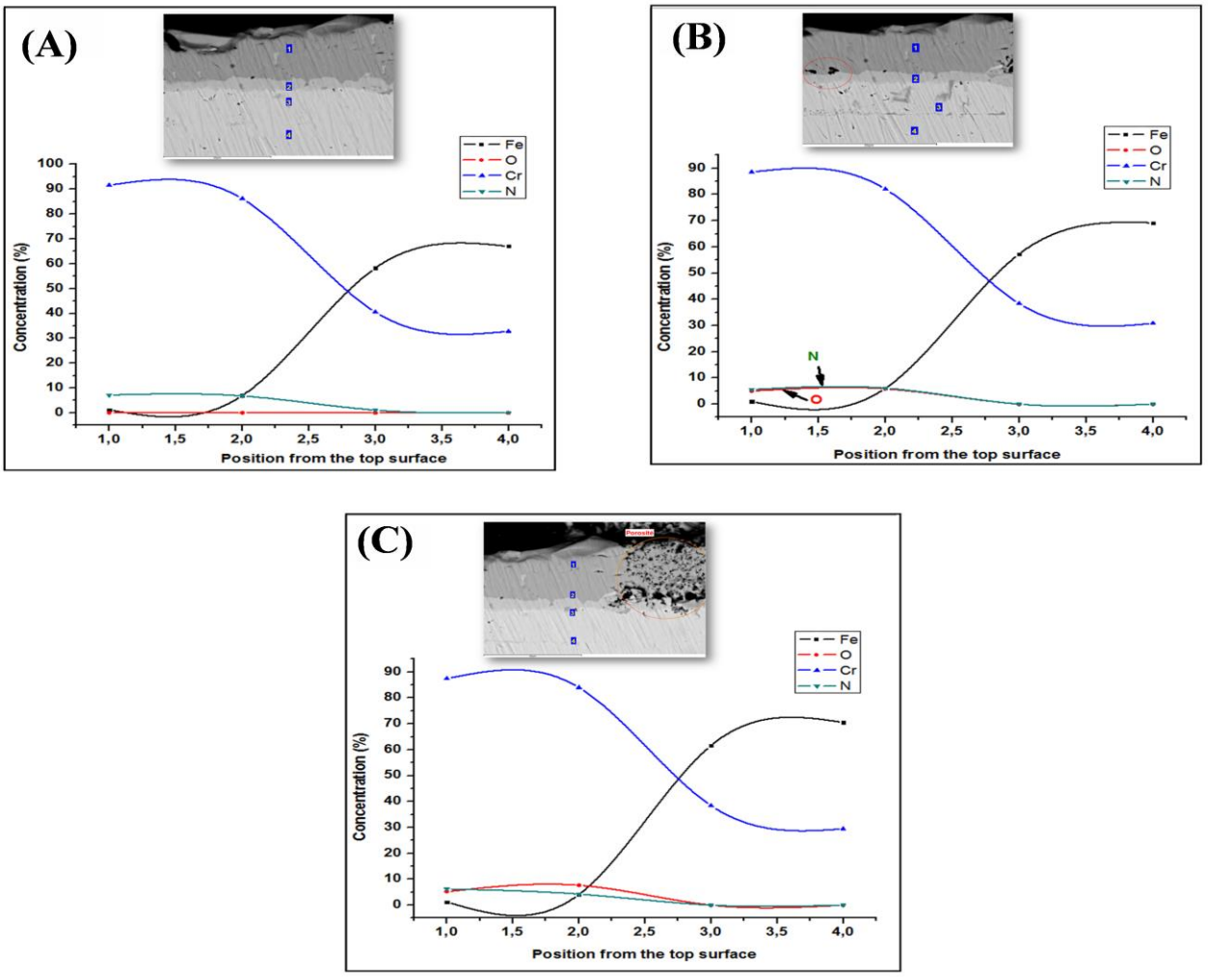

Fig. 6. Concentration profiles of iron, oxygen, nitrogen and chromium across the doped interfaces: (A) Cr-Mg/1 wt.%; (B) Cr-Mg/2 wt.%; (C) Cr-Mg/3 wt.%.

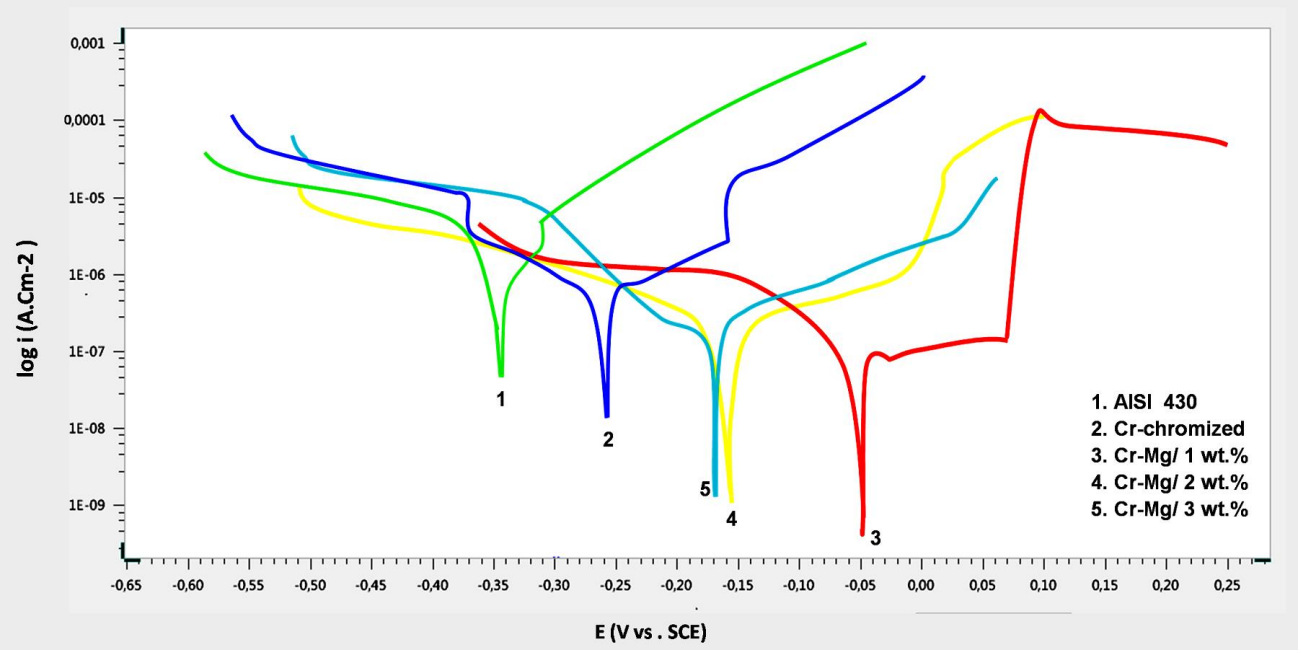

Fig. 7. Superposition of polarization curves for different coatings in 3.5% NaCl solution. The substrate AISI 430 and the chromized non-doped coating were also plotted.

saline solution creates an environment where the corrosion rate is extremely low, typically associated with the passive corrosion. It is important to note that the Cr-Mg/ 1 wt.% doped layer exhibits the largest capacitive loop and the most important resistance (Rs, 1429 Ω.Cm^{-2} and Rp, 96893 Ω) compared to those recorded for the Cr-Mg/ 2 wt.% and Cr- Mg/ 3 wt.% coatings, where Rs values were 357 Ω.Cm^{-2} and 184 Ω.Cm^{-2}, respectively.

Table 3

Electrochemical parameters derived from the polarization curves for the different doped coatings in 3.5% NaCl solution

Parameters / Substrates	Ecorr mV/SCE	Icorr µA/cm^2	βa mV/dec	βc mV/dec
Cr-Mg/ 1wt.%Mg	-52.16	0.003	241.53	94.24
Cr-Mg/ 2wt.%Mg	-157.29	0.008	108.98	67.76
Cr-Mg/ 3wt.%Mg	-178.18	0.219	172.53	99.83

The results may explain the resistance to the propagation of chloride ions (Cl^-) of all the surfaces, but the doped layer with 1 wt.% Mg showed the excellent resistance. Analyzing the data compiled in Table 4 and the diagrams plotted in Fig. 9, we can notice a significant improvement in electrochemical behavior, where the values of resistance Rs and Rp increase with Mg content increase to 1 wt.% and 2 wt.%, remaining moderate for 3 wt.% Mg. This signifies that doping, by enhancing surface chromium diffusion and enhancing surface characteristics, could improve corrosion resistance and prevents chloride ions (Cl-) from moving and propagating through the Cr-Mg doped layer. Furthermore, the capacity of the Cr-doped layer decreases with corrosion rate. This capacity reflects the way in which the chromized-doped layer is able to store Cl- charges. However, the capacity (C_{dc}) is found to increase by increasing the Mg content, where Cr-Mg/ 3 wt.% showed the higher value of about 26.61 µF. This is likely due to the presence of network of pores and non-crystalline areas (as confirmed by SEM analysis, sowed in Fig. 5), which facilitates Cl^- ion storage at the surface by creating path ways for these corrosive agents.

Table 4

Kinetic parameters deduced from impedance curves of surfaces coated in my 3.5% NaCl solution.

Parameters / Substrate	Rs (Ω.Cm^{-2})	Rp (Ω.Cm^{-2})	C_{dc} (µF)
Cr-Mg/ 1wt.%	1429	96893	1.429
Cr-Mg/ 2wt.%	357.46	42562	10.61
Cr-Mg/ 3wt.%	184.1	28092	26.61

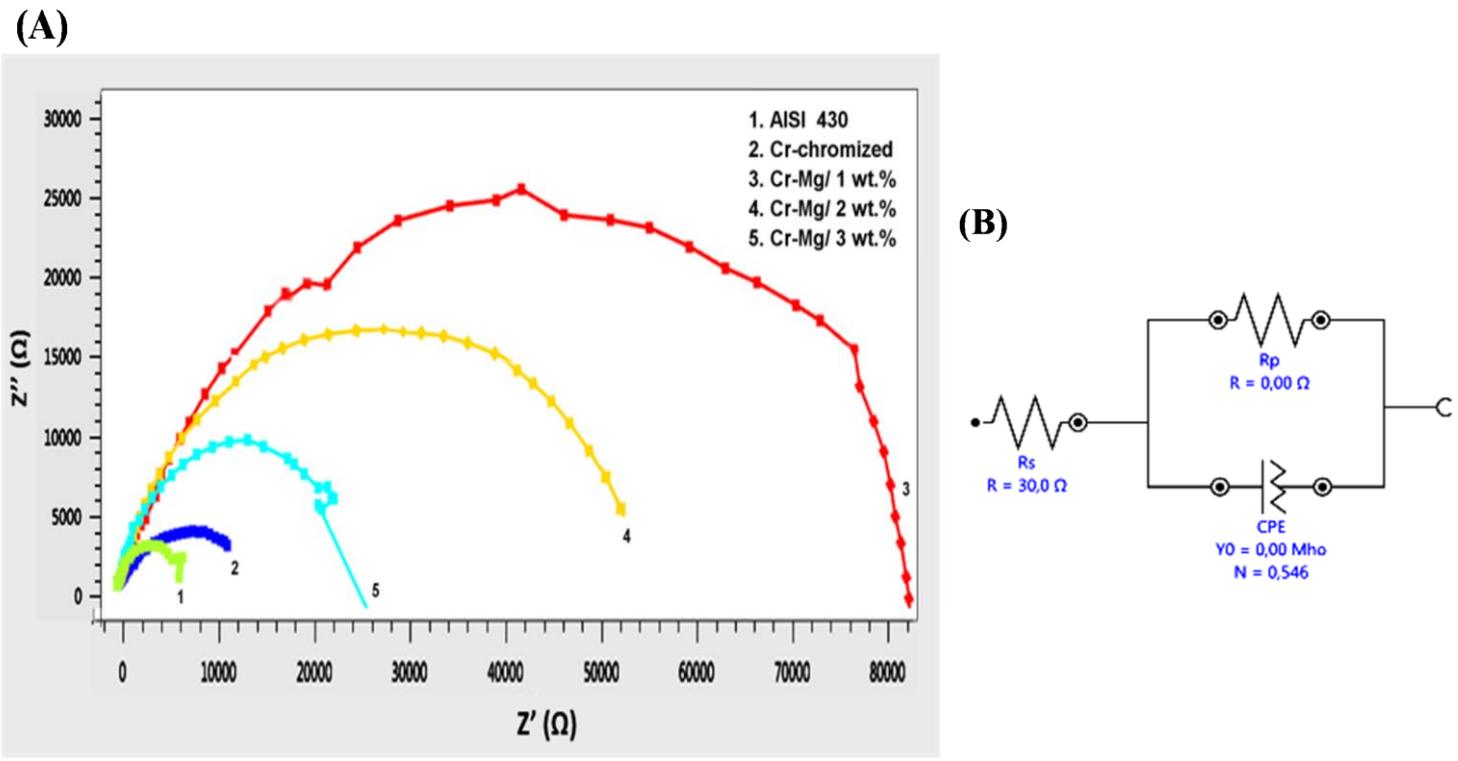

Fig. 8. (A) Nyquist impedance diagrams for different Mg chromized-doped coatings in 3.5% solution. The substrate and the non-doped coating were also plotted. (B) Electrical equivalent circuit employed for impedance fitting.

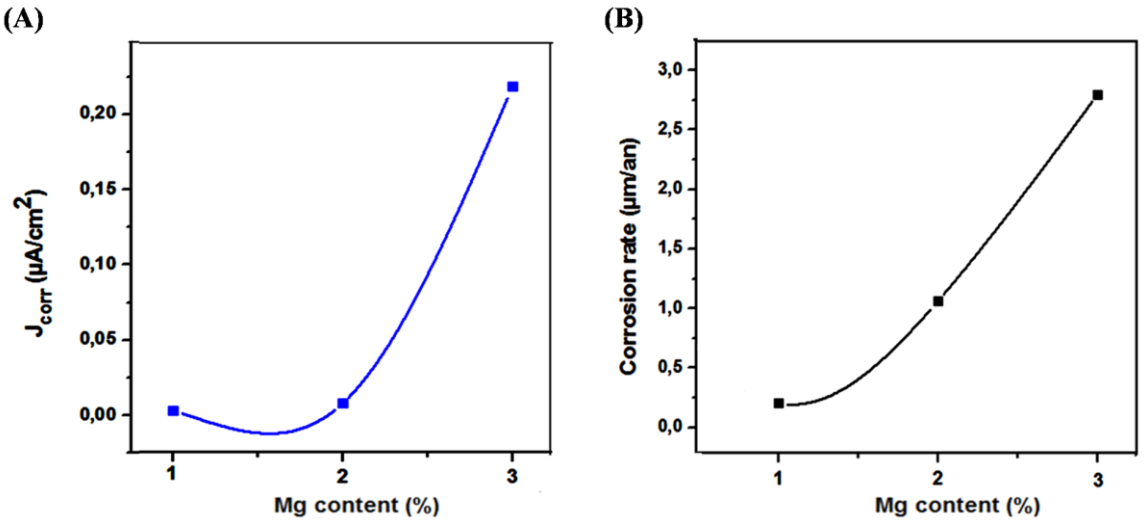

Fig. 9. Electrochemical impedance spectroscopy data of coatings: (A) corrosion rate, (B) corrosion current density.

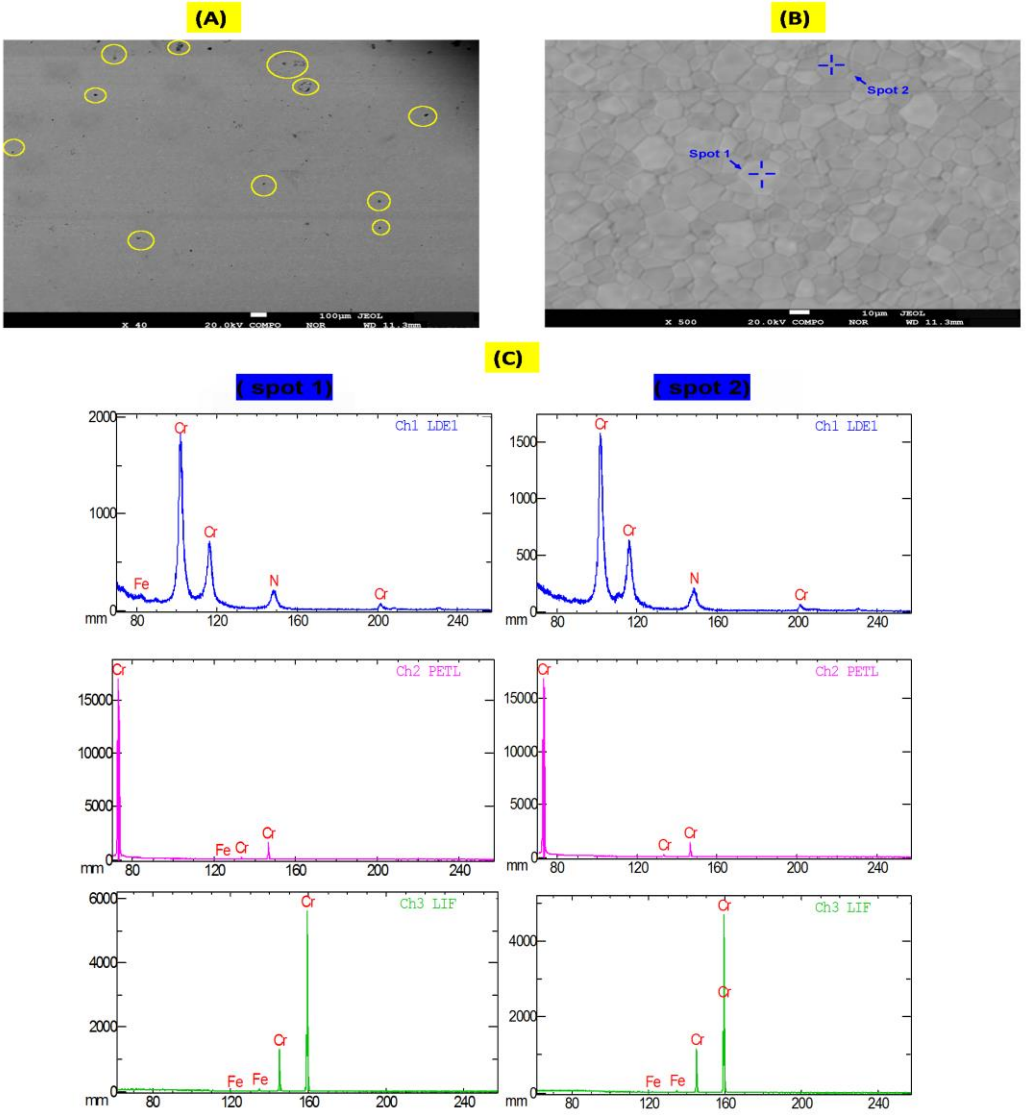

Fig. 10. EPMA analysis of the surface of Cr-Mg/1 wt.% after polarization test in 3.5 % NaCl: (A, B) Surface topographies; (C) Elementary distribution analysis of the resulted corrosion products in spot 1 and spot 2.

This accelerates the corrosion phenomena and resulting in a higher corrosion rate, as confirmed for the 3 wt.% Mg doped-chromized coating (2.8023 µm/year). In contrast, Cr-Mg/1 wt.% layer exhibited the lowest corrosion rate, around 0.1778 µm/year.

3.3 Analysis of the surfaces after corrosion test (EPMA)

For a better understanding of the composition, the nature of the products formed and the reactions that have been produced after immersing the chromized-doped surfaces in a 3.5% NaCl solution, we employed electron probe microanalysis (EPMA) to analyze the topography and the elementary composition. Fig. 10 illustrates the morphology of the surface of the Cr-Mg/1 wt.% immersed in 3.5% NaCl solution. Initially, we spotted small inclusions that seemed to suggest a non-significant corrosion pitting at low- magnification observations. However, what is particularly interesting is that when we increased the magnification of the EPMA, these inclusions became totally invisible and disappeared (Fig.10-B).This could explain that the inclusions do not propagate deeply into this chromized-doped coating; hence they couldn't reach the top surface and the interlayer. The overall surface morphology remained unchanged from its initial state (Fig. 3), retaining a smooth crystalline structure without a significant porosity formation and absence of microcracks or other damages. Additionally, a variation in the color within these grains was observed. Some grains appeared light gray, while others remained a dark gray. In light of this observation, the areas of the grain were analyzed to evaluate the developed composition inside. The results revealed that the grains, referred to as 'spot 1' and 'spot 2' during analysis, had a similar composition (Fig. 10 -C). It is composed of significant major proportions of metallic chromium (Cr) and minor proportions nitrogen (N) contents. The surfaces exhibited no traces of oxygen (O), chloride (Cl) or sodium (Na), which could explain that they did not suffer any type of corrosion or damage. Moreover, this could explain that chromium nitrides Cr_2N and rich areas of metallic chromium (Cr) are highly corrosion-resistant, hence hard substances. Li et al. [24] concluded in their work that chromium nitrides (Cr_2N) remained the microstructure dense, which systematically enhances surface corrosion resistance. They effectively prevent chloride ions (Cl^-) and oxygen (O) from interacting with the surface when no defects such as porosity, voids, and material detachment are present. These results may clarify why the unchanged morphology of the coating (Fig.10–B) (compared to its initial state) was observed, even after exposure to this corrosive environment and in presence of chloride (Cl^-) ions.

Furthermore, the surfaces of Cr-Mg/ 2 wt.% and Cr- Mg/ 3 wt.% after polarization tests are represented in Fig.11 and

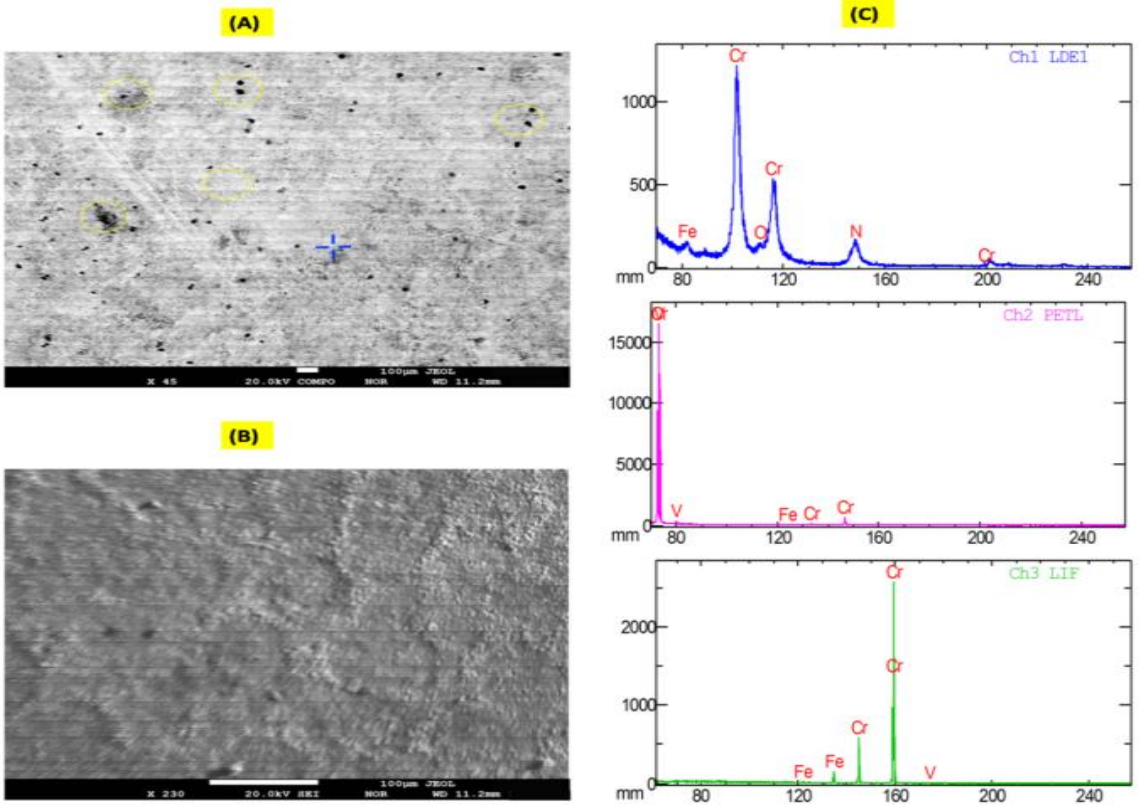

Fig. 11. EPMA analysis of the surface of Cr-Mg/2 wt.% after polarization test in 3.5 % NaCl: (A, B) Surface topographies; (C) Elementary distribution analysis of corrosion products.

Fig.12, respectively. Both of the chromized-doped coatings exhibited apparent surface more rough than that of Cr-Mg/1 wt.% after corrosion tests (Fig.10-A and Fig.11- A), along with small particles and inclusions that also have been observed. The inclusions became invisible as the observation magnification increased but they stilled insignificant. Thus, the particles remained visible, although their density on the surface of the Cr-Mg/ 2 wt.% doped coating (Fig.11-B) was lower than that of the Cr-Mg/3wt.% (Fig.12-B). These results could indicate that the corrosion resistance is systematically related to the content of Mg and NH_4Cl in the pack mixture, which is found to cause the apparition of defects on the top layer. However, the depth of the inclusions is not significant, indicating no significant damage to their surfaces. Composition analysis suggests that both of chromized-doped coatings have developed a tinny layer of chromium oxide (Cr_2O_3) since oxygen (O) peaks were detected with contents of 5.33% and 11.44% for Cr-Mg/2 wt.% and Cr-Mg/3wt.% doped coatings, respectively. Despite the presence of chromium nitrides (Cr_2N), which improve corrosion resistance, the formation of chromium oxide (Cr_2O_3) on the surface of Cr-Mg/3 wt.% could be explained by an interaction between the layer and chloride ions (Cl-). Due to the formation of chromium oxide and the limitation of these ions to propagate through pores and voids and non-crystalline areas present in the layer, this interaction was not really significant and did not cause a major defect to the surface of the Cr-Mg/3wt.%. Its less resistance than the other coatings could be attributed to the presence of defects that were caused by the decreased of activator in the pack mixture. On the other hand; the doped layers are considered stable after doping, where the degradation is not speed according to the results of the rate corrosion illustrated in Fig. 9, and the absence of other substances as iron oxides. Despite this, a more important degradation was identified for the Cr-Mg/ 3 wt.%, where it is related to the presence of pores and some voids in its interlayer caused by the high content of Mg than the other doped layers, especially the Cr-Mg/ 1 wt.%. Despite the presence of defects, the $MgCr_2O_4$ oxide could prevent the rapid propagation of Cl^- ions through these defects. Based on EDX analysis of cross-sections of submerged surfaces shown in Fig. 13, the chromium content after polarization is considered stable for Cr-Mg/1 wt. % layer and oxygen is completely absent. Whereas, the other layers showed the presence of small quantities of oxygen and the consumption of chromium, especially for the Cr-Mg/ 3 wt.%. This could confirm the formation of a stable chromium protective layer that did not develop rapidly, which it is consistent with the corrosion rate shown in the Table 4.

3. Conclusion

As a conclusion, we summarize our observations and findings

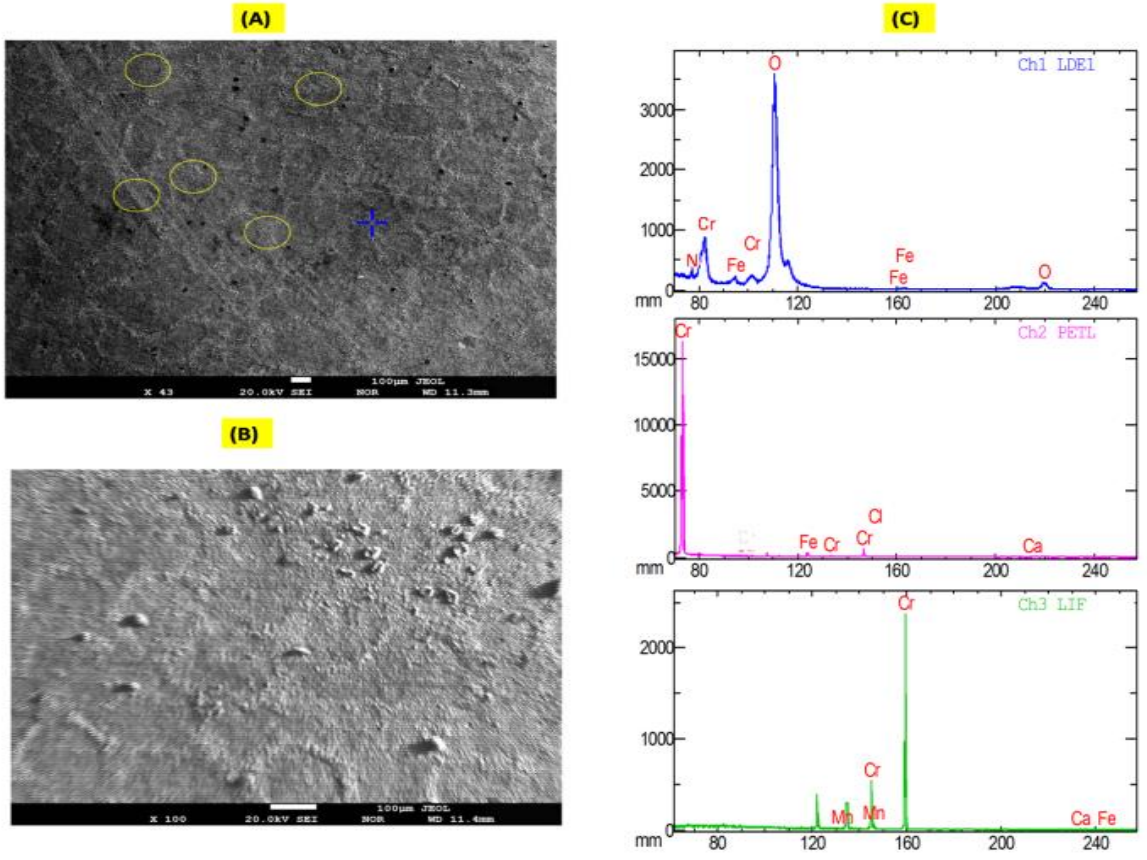

Fig. 12. EPMA analysis of the surface of Cr-Mg/3 wt.% after polarization test in 3.5 % NaCl: (A, B) Surface topographies; (C) Elementary distribution analysis of the products resulted after corrosion testing.

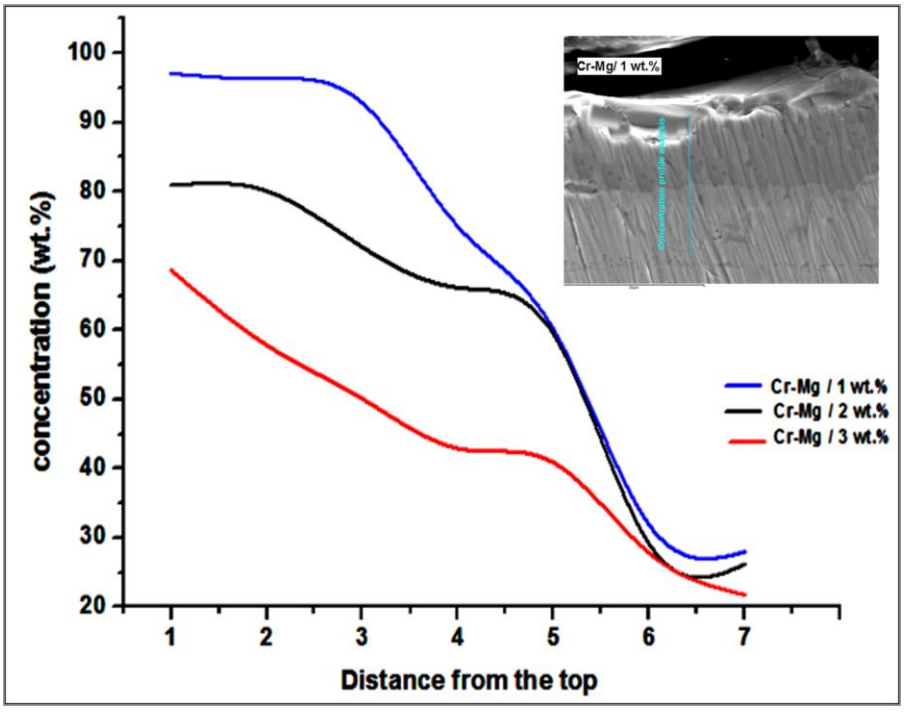

Fig. 13. Chromium concentration profiles of the doped-chromized layers after polarization test in 3.5 % NaCl.

regarding the original problem statement, namely determining how variations in Mg doping elements and employed activator affect the microstructural and electrochemical properties of the chromized layer, so as the stability of the formed layer, formed chromine and the diffusion process :

The chromized layer was successfully doped with magnesium by incorporating small amounts of 1 wt.%, 2 wt.%, and 3 wt.% in the powder mixture, showing a proportional relationship with ammonium chloride (NH_4Cl) activator. However, a crystalline microstructure (absence of fine particles or microcracks) was observed on all the chromized-doped surfaces, which increased in size as Mg content increased. Doping the layer with 1 wt.% Mg revealed a more smoother surface within significant defects, while higher concentrations (2 wt.% Mg and 3 wt.% Mg) exhibited pores and voids due to the kirkendall effect caused by the decrease of NH_4Cl activator in the powder mixture. A development of non-crystalline regions for the doped layers with 2 wt.% Mg and 3 wt.% Mg was observed, which suggest that doping with this concentration could affect the morphology and the quality of the layer. Additionally, when 2 wt.% Mg and 3 wt.% Mg were applied with a decreased activator; a lower content than that used for 1 wt.% Mg, the growth rate slowed and the diffused chromium concentration at the surface decreased. As a result, $MgCr_2O_4$ oxide forms during the slow diffusion process, where the Mg content could react with the chromium oxide formed, inhibiting its formation and resulting in the more stable chromium oxide. The Cr-Mg/1 wt.% revealed the high diffusion chromium, reaching approximately 98 % on the surface, while chromium content at the depth was about of 32 %, which it could be considered as an improvement of Chromium diffusion.

This study has highlighted a remarkable and noteworthy corrosion resistance in 3.5% NaCl for all the doped layers even with the presence of some defects on their surfaces. Nevertheless, the results revealed that the doped layer with 1 wt.% Mg exhibited the least negative corrosion potential and the highest resistance (Rs) of 1429 Ω/cm^2, indicating an important corrosion resistance than the other layers. Similarly, the doped with 2 wt.% Mg and 3 wt.% Mg showed substantial corrosion potentials, attesting to their corrosion resistance capabilities, while their Rs values were very lower compared to the chromized-doped with 1wt.% Mg. This could be attributed to defects present on their surfaces, particularly voids likely caused by the reduction of ammonium chloride (NH_4Cl) activator, despite the presence of a stable layer containing $MgCr_2O_4$ oxide. According to the results of EPMA and EDX analysis, the doped layer with 1 wt.% Mg revealed unchanged from its initial state before electrochemical testing and proved to be the most effective in terms of corrosion resistance. It showed stable chromium content after electrochemical testing more than that found for the other layer, especially the doped with 3 wt.% Mg, which noticed the presence of protective layer formed under Cl^- ions attack through the pores and the defects in its surface. It is worth noting that the parameters used for 1wt.% doping could be the optimal parameters for reaching a layer with high and stable quality, chromium diffusion, and corrosion resistance in a 3.5% NaCl environment.

Author contributions D.S. and V. M. contributed to conceptualization; D.S., V. M., M.Y., D.A., H.A., and B.H. contributed to investigations and software; D.S. and M.Y. contributed to methodology; D.S., V. M., M.Y., and H. A. contri-

buted to supervision; D.S., V.M., and M.Y contributed to validation; D.S., V. M., M.Y., D.A., H.A., and B. H. contributed to writing—original draft preparation; D.S., V.M contributed to writing—review & editing.

Funding The authors acknowledge that no specific grants or financial assistance were received in the development and completion of this work.

Conflict of interest In this paper, the authors declare that they have no competing financial interests or personal relationships that could have influenced their scientific work.

Data availability Research described in this article did not use any data.

References

[1] Lee S, Cho K, Lee W and Jang H 2009 Improved corrosion resistance and interfacial contact resistance of 316 l stainless-steel for proton exchange membrane fuel cell bipolar plates by chromizing surface treatment, *Journal of Power Sources*. 187: 318-323. https://doi.org/10.1016/j.jpowsour.2008.11.064

[2] Colas R, and Totten G E 2016 Encyclopedia of iron, steel, and their alloys (Online version) (1st ed.), *CRC Press*. 4238. https://doi.org/10.1081/E-EISA

[3] Li H 2017 Stability of Mn-Cr-O Spinel and Chromium Oxide in High Temerature Ethylene Cracking Environments. *Doctoral dissertation*. University of Alberta.

[4] Syamimi A K, Wahab H M A, and Abdullah T K. 2019 High temperature isothermal oxidation behavior of superheater materials. *Materials Today: Proceedings.* 17: 829-835. http://dx.doi.org/10.1016/j.matpr.2019.06.369

[5] Meng T, Guo Q, Xi W, Ding W, Liu X, Lin N, Yu S and Liu X 2018 Effect of surface etching on the oxidation behavior of plasma chromizing-treated aisi 440b stainless steel. *Applied Surface Science.* 433: 855-861. https://doi.org/10.1016/j.apsusc.2017.10.111

[6] Bai C Y, Lee J L, Wen T M, Hou K H, Wu M S and Ger M D 2011 The characterristics of chromized 1020 steel with electrical discharge machining and Ni electroplating pretreatments. *Applied Surface Science*. 257: 3529-3537. https://doi.org/10.1016/j.apsusc.2010.11.070

[7] Hu J, Zhang Y, Yang X, Li H, Xu H, Ma C, Dong Q, Guo N and Yao Z 2018 Effect of pack-chromizing temperature on microstructure and performance of AISI 5140 steel with Cr-coatings. *Surface and Coatings Technology*. 344: 656-663. https://doi.org/10.1016/j.surfcoat.2018.03.099

[8] LIN N, XIE F, YANG H, et al 2012 Assessments on friction and wear behaviors of P110 steel and chromizing coating sliding against two counterparts under dry and wet conditions. *Applied Surface Science*. 258: 4960-4970. http://dx.doi.org/10.1016/j.apsusc.2012.01.128

[9] Wang Z, Lu J. and Lu K 2006 Wear and corrosion properties of a low carbon steel processed by means of smat followed by lower temperature chromizing treatment. Surface *and Coatings Technology*. 201: 2796-2801. https://doi.org/10.1016/j.surfcoat.2006.05.019

[10] LIU W, XUE L, DI J, Zhou Q, Zhang H, Li H, and Yan Y 2021 An efficient graphene oxide reinforced aluminum phosphate/Cr2O3 double coating as an enhanced tritium permeation barrier. *Surface and Coatings Technology*. 405: 126699. https://doi.org/10.1016/j.surfcoat.2020.126699

[11] Djemmah S, Madi Y, Voué M, Haddad A, Allou D, Oualllam S, et al 2023 Effect of Mg Addition on Morphology, Roughness and Adhesion of Cr Chromized Layer Produced by Pack Cementation. International *Journal of Engineering, Transactions A: Basics*. 36: 1773-1782. http://dx.doi.org/10.5829/IJE.2023.36.10A.05

[12] Fentazi S, Bournane M, Sadaoui Y, Boutemeur M 2017 Effet de la teneur en magnésium sur les propriétés mécaniques des alliages de fonderie B206. *13ème édition du congrès de mécanique CMM*.

[13] Holt A, and KOFSTAD P 1997 Electrical conductivity and defect structure of Mg-doped Cr2O3. *Solid State Ionics*. 100: 201-209. https://doi.org/10.1016/S0167-2738(97)00352-4

[14] Arca E, Kehoe A B, Veal T D, Shmeliov A, Scanlon D O, Downing C, and Watson G W 2017 Valence band modification of Cr 2 O 3 by Ni-doping: creating a high figure of merit p-type TCO. *Journal of Materials Chemistry C* 5: 12610-12618. https://doi.org/10.1039/C7TC03545D

[15] Han D, Hou Y, Jiang B, Geng B, He X, Shagdar E, Lougou B G and Shuai Y 2023 Enhanced corrosion resistance of alloy in molten chloride salts by adding nanoparticles for thermal energy storage applications. *Journal of Energy Storage*. 64: 107172. https://doi.org/10.1016/j.est.2023.107172

[16] TANG X, WANG S, QIAN L, Ren M, et al 2016 Corrosion properties of candidate materials in supercritical water oxidation process. Journal *of Advanced Oxidation Technologies.* 19: 141-157. http://dx.doi.org/10.1515/jaots-2016-0119

[17] Chen J K, Chen S F, and Huang C S 2012 Formation of Al and Cr dual coatings by pack cementation on SnCN439 steel. *ISIJ International.* 52. http://dx.doi.org/10.2355/isijinternational.52.127

[18] Park h Ho, Lee K T and Shin H S 1998 Simultaneous chromizing-aluminizing diff-usion coating of austenitic stainless steel by a two-step CVD process. *Oxidation of metals.* 50: 377–387. https://doi.org/10.1023/A:1018800723939

[19] Wen T M, Hou K H, Bai C Y, Ger M D, Chien P H, and Lee S J 2010 Corrosion behaviour and characteristics of reforming chromized coatings on SS 420 steel in the simulated environment of proton exchange membrane fuel cells. *Corrosion science.* 52: 3599–3608. https://doi.org/10.1016/j.corsci.2010.07.005

[20] Wang S, Liu P 2016 The technology of preparing green coating by conducting micro-arc oxidation on az91d magnesium alloy. *Polish Journal of Chemical Technology*. 18: 36–40. https://doi.org/10.1515/pjct-2016-0068

[21] Fedorchenko I M, Slys I G, Sosnovskii L A 1972 Technology of sintering of powder metallurgical materials without a circulating protective atmosphere. *Soviet Powder Metallurgy and Metal Ceramics.* 11: 361–366. https://doi.org/10.1007/BF00797738

[22] Du C, Zuo K, Ma Z, Zhao M, Li Y, Tian S, Lu Y, Xiao G 2022 Effect

of substrates performance on the microstructure and properties of phosphate chemical conversion coatings on metal surfaces. *Molecules.* 27: 6434. https://doi.org/10.3390/molecules27196434

[23] Miller E L, Thompson S T, Randolph K, Hulvey Z, Rustagi N, Satyapal S 2020 Us department of energy hydrogen and fuel cell technologies perspectives. *MRS Bulletin.* 45: 57–64. https://doi.org/10.1557/mrs.2019.312

[24] Li Y, He Y, Xiu J, Wang W, Zhu Y, Hu B 2017 Wear and corrosion properties of AISI 420 martensitic stainless steel treated by active screen plasma nitriding. *Surface and Coatings Technology.* 329: 184–192. https://doi.org/10.1016/j.surfcoat.2017.09.021